

Scientific paper

Synthesis, Structural Diversity and Mimic Superoxide Dismutase of Mn(II) Complexes Derived from N, O-donor Schiff bases

Jie Qin,* Qiang Yin, Shan-Shan Zhao, Jun-Zheng Wang and Shao-Song Qian*

School of Life Sciences, Shandong University of Technology, Zibo 255049, P. R. China

* Corresponding author: E-mail: qinjietutu@163.com, sdutqss@163.com

Tel.: 0086-533-2780271; Fax: 0086-533-2781329

Received: 18-08-2015

Abstract

Two new potentially tetradentate Schiff base ligands *N'*-(pyridin-2-ylmethylene)nicotinohydrazide (L_1), and *N'*-(pyridin-2-ylmethylene)isonicotinohydrazide (L_2) were synthesized. Reactions of hydrazone ligands L_1 and L_2 with $\text{Mn}(\text{NO}_3)_2$ afford two mononuclear Mn(II) complexes, $[\text{Mn}(L_1)(\text{NO}_3)(\text{H}_2\text{O})_2]\text{NO}_3$ (**1**) and $[\text{Mn}(L_2)_2(\text{NO}_3)(\text{H}_2\text{O})]\text{NO}_3$ (**2**). For complexes **1** and **2**, L_1 and L_2 act as pincer-like tridentate or bidentate ligands, respectively. The Mn(II) ions in the two compounds are both in hepta-coordinated environment, while the two molecules display diverse solid-state supramolecular structures because of the different orientation of $\text{N}_{\text{pyridine}}$ and hydrogen bonding patterns of nitrate anions. Complex **1** features 2D supramolecular sheet, while complex **2** has double-chain supramolecular structure. Both of the complexes exhibit moderate superoxide dismutase (SOD) mimetic activity.

Keywords: Schiff base; Mn(II) complex; Supramolecular structure; SOD mimetic activity

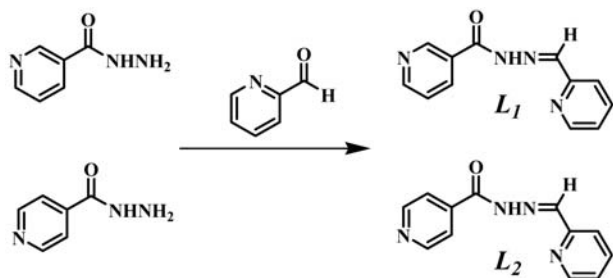
1. Introduction

Schiff base compounds derived from the condensation reaction of aldehydes with amines are very attractive for their coordination ability to metal atoms,^{1–3} and excellent biological applications.^{4,5} Among the variety of aldehydes, salicylaldehyde derivatives are mostly used. Within this form of aldehydes, a number of bidentate NO or tetradentate N_2O_4 Schiff base ligands have been used as the building blocks to obtain a variety of coordination complexes.^{6–8} Aygün et al. have also reported tridentate Schiff base ligand derived from phenylalanine and 2,4-dihydroxybenzaldehyde.⁹ While Schiff base ligands based on pyridylaldehyde derivatives are still rare or lacking.^{10,11} Aroyl hydrazones are an important class of Schiff base ligands, coordinating through amide oxygen and the imine nitrogen of hydrazone moiety.^{10,12} Moreover, N and O heteroatoms of the aroyl hydrazones with free electron pairs can also be considered as potential hydrogen bond acceptors to expand polymeric frameworks with hydrogen-bonding interactions.

Numerous diseases, such as amyotrophic lateral sclerosis, Parkinson's disease, Alzheimer's disease are

considered to be connected with the over production of superoxide radical anion. Superoxide dismutase (SOD) can accelerate the dismutation of superoxide anion into hydrogen peroxide and dioxygen, which play an important role in defending life from the diseases mentioned above.¹³ Three isoforms of SOD have been found, including Cu/Zn-SOD (SOD 1), Mn-SOD (SOD 2) and extracellular SOD (SOD 3). Compared with native SOD enzymes, low molecular weight SOD mimics have advantages in lack of immunogenic responses, improved access to lipid layer of the cell membrane, and low cost.¹⁴ Therefore the rational design and synthesis of SOD mimics has potential in metal-based therapeutic agents. Mn complexes derived from Schiff base, porphyrin and their derivatives have been studied as Mn-SOD mimics.¹⁵

In this contribution, we present the synthesis of two new hydrazone Schiff base ligands *N'*-(pyridin-2-ylmethylene)nicotinohydrazide (L_1) and *N'*-(pyridin-2-ylmethylene)isonicotinohydrazide (L_2) (see Scheme 1), and two novel mononuclear Mn(II) complexes **1** and **2** generated from these two hydrazone ligands and $\text{Mn}(\text{NO}_3)_2$, the structures and IR spectra, as well as the SOD mimetic activities.



Scheme 1. Synthetic routes to hydrazone ligands.

2. Experimental

2.1. Physical Measurements and Materials

All the solvents and reagents were reagent grade and used as received. Nicotino-hydrazone, isonicotino-hydrazone, 2-pyridinecarboxaldehyde, and $\text{Mn}(\text{NO}_3)_2 \cdot 4\text{H}_2\text{O}$ were purchased from Aladdin Industrial Corporation (China). Superoxide Dismutase Assay Kit was purchased from Nanjing Jiancheng Bioengineering Insitute (China). N' -(pyridin-2-ylmethylene)nicotino-hydrazone (L_1) and N' -(pyridin-2-ylmethylene)isonicotino-hydrazone (L_2) were synthesized according to the literature.¹⁶ The IR spectra were taken on a Vector 22 Bruker spectrophotometer ($400\text{--}4000\text{ cm}^{-1}$) with KBr pellets. Elemental analyses for C, H and N were performed on a Perkin-Elmer 240C analyzer. ^1H NMR spectra were measured on a Bruker AM 500 spectrometer.

2.2. X-ray Crystallography

Diffraction intensities for complexes **1** and **2** were collected at 298 K on a Bruker Smart Apex CCD diffractometer equipped with graphite-monochromated Mo $K\alpha$ ($\lambda = 0.71073\text{ \AA}$) radiation using a ω - 2θ scan mode. The collected data were reduced using the SAINT program,¹⁷ and multi-scan absorption corrections were performed using the SADABS program.¹⁸ The structures were solved by direct methods and refined based on F^2 by full-matrix least-squares methods were performed with the SHELXTL program packages.¹⁹ All non-hydrogen atoms were refined with anisotropic displacement parameters. All the hydrogen atoms bonded to C atoms were generated geometrically and refined isotropically using the riding model. While hydrogen atoms bond to N or O atoms were first found in the Fourier map and then fixed at their ideal positions. Water H atoms were refined with distance restraints of $\text{O}\text{--}\text{H} = 0.85(1)\text{ \AA}$, $\text{H}\cdots\text{H} = 1.44(2)\text{ \AA}$ and $U_{\text{iso}}(\text{H}) = 1.5U_{\text{eq}}(\text{O})$. Imine H atoms were refined with distance restraints of $\text{N}\text{--}\text{H} = 0.89(1)\text{ \AA}$, and $U_{\text{iso}}(\text{H}) = 1.5U_{\text{eq}}(\text{N})$. In complex **2**, O5 was disordered over two positions that refined to a ratio of 0.50(4):0.50(4). Further refinement details of the structural analysis for the two complexes are given in Table 1. Selected bond lengths and angles of the complexes are listed in Table 2.

Table 1. Crystallographic data for complexes **1** and **2**.

	1	2
Chemical formula	$\text{C}_{12}\text{H}_{14}\text{MnN}_6\text{O}_9$	$\text{C}_{24}\text{H}_{22}\text{MnN}_{10}\text{O}_9$
Formula Weight	441.23	649.46
Crystal System	Triclinic	Triclinic
Space group	$P\bar{1}$	$P\bar{1}$
Temperature (K)	298	298
a (\AA)	8.6450 (17)	9.1500 (4)
b (\AA)	9.5075 (17)	10.4018 (5)
c (\AA)	10.8250 (18)	14.4785 (6)
α ($^\circ$)	82.180 (5)	83.173 (1)
β ($^\circ$)	88.184 (6)	86.514 (1)
γ ($^\circ$)	89.803 (6)	89.360 (2)
V (\AA^3)	881.0 (3)	1365.70 (11)
Z	2	2
μ (Mo- $K\alpha$)(mm^{-1})	0.812	0.556
R_1, wR_2 [$I > 2\sigma(I)$]	0.167, 1.05	0.122, 1.03
ρ_c (g cm^{-3})	1.663	1.579
$F(000)$	450	666
Goodness of fit on F^2	1.05	1.03

2.3. Superoxide Dismutase Assay

The SOD activity of the title complexes was studied by indirect method using Superoxide Dismutase Assay Kit according to the instruction of the manufacturer. Briefly, the xanthine-xanthine oxidase system was used for the production of superoxide. For the detection of superoxide the absorbance increases at 510 nm arising from the reduction of iodophenyl nitrophenyl phenyltetrazolium salt (INT). The reaction mixture contained $4.2 \cdot 10^{-5}\text{ M}$ xanthine and $8.25 \cdot 10^{-5}\text{ M}$ INT in 0.05 M phosphate buffer solution at pH 7.8. The reaction was started by the addition of xanthine oxidase in the amount needed to generate the absorbance change 0.03–0.04 min^{-1} . The SOD mimic activity of the complexes **1** and **2** was evaluated from the absorbance decrease comparing to the blank after the 10 min incubation at 37 $^\circ\text{C}$. The IC_{50} value was defined as the concentration of complex (μM) necessary for the 50% inhibition of the INT reduction.

2.4. Synthesis of $[\text{Mn}(L_1)(\text{NO}_3)(\text{H}_2\text{O})_2]\text{NO}_3$ (**1**)

A solution of $\text{Mn}(\text{NO}_3)_2 \cdot 4\text{H}_2\text{O}$ (16.1 mg, 0.050 mmol) in EtOH (5 mL) was layered onto a solution of L_1 (9.1 mg, 0.040 mmol) in CH_2Cl_2 (5 mL). The system was left for about one week at room temperature, after which time crystals of **1** were obtained (yield 61%). IR (KBr, cm^{-1}): 3350, 3220, 3066, 1648, 1598, 1556, 1495, 1474, 1443, 1381, 1303, 1225, 1158, 1136, 1111, 1027, 1010, 959, 922, 823, 785, 735, 700, 637, 522. Anal. Calcd. for $\text{C}_{12}\text{H}_{14}\text{MnN}_6\text{O}_9$ (%): C, 32.67; H, 3.19; N, 19.05. Found: C, 32.75; H, 3.17; N, 19.11.

2. 5. Synthesis of $[\text{Mn}(L_2)_2(\text{NO}_3)(\text{H}_2\text{O})\text{NO}_3]$ (2)

Complex **2** was synthesized in an analogous manner, but using L_2 instead of L_1 . Yield 53%. IR (KBr, cm^{-1}): 3383, 3178, 3051, 1645, 1599, 1553, 1487, 1470, 1443, 1384, 1313, 1254, 1219, 1153, 1106, 1060, 1037, 1006, 923, 850, 784, 751, 731, 692, 683, 632, 589, 522. Anal. Calcd. for $\text{C}_{24}\text{H}_{22}\text{MnN}_{10}\text{O}_9$ (%): C, 44.38; H, 3.41; N, 21.57. Found: C, 44.51; H, 3.39; N, 21.63.

3. Results and Discussion

3. 1. Synthesis

Ligand L_1 and L_2 was synthesized by a one-pot condensation reaction of nicotinohydrazide or isonicotinohydrazide with pyridine-2-carboxaldehyde in ethanol solution at refluxing temperature, respectively. The products were washed with cold ethanol. Mononuclear metal complexes **1** and **2** were obtained by coordination of L_1 or L_2 with $\text{Mn}(\text{NO}_3)_2 \cdot 4\text{H}_2\text{O}$ at room temperature, respectively. Their IR and ^1H NMR spectra were depicted in Figures S1–S4.

Table 2. Selected bond angles ($^\circ$) and bond lengths (\AA) for **1** and **2**.

	1		2
Mn1–O9	2.178(3)	Mn1–O9	2.1666(17)
Mn1–O8	2.197(3)	Mn1–O3	2.228(2)
Mn1–O3	2.382(3)	Mn1–O2	2.2679(15)
Mn1–O2	2.249(3)	Mn1–O1	2.4148(16)
Mn1–O1	2.354(3)	Mn1–N6	2.3594(19)
Mn1–N1	2.333(3)	Mn1–N1	2.3915(17)
Mn1–N2	2.267(3)	Mn1–N2	2.2894(18)
O9–Mn1–O8	177.47(11)	O9–Mn1–O3	164.05(7)
O9–Mn1–N1	94.16(11)	O9–Mn1–O2	83.15(6)
O9–Mn1–N2	89.37(11)	O9–Mn1–O1	82.92(6)
O9–Mn1–O1	88.43(10)	O9–Mn1–N1	87.11(7)
O9–Mn1–O3	90.83(12)	O9–Mn1–N2	94.51(6)
O9–Mn1–O2	87.07(11)	O9–Mn1–N6	91.94(7)
N2–Mn1–N1	70.11(11)	O2–Mn1–N1	80.67(6)
N2–Mn1–O1	68.32(10)	N2–Mn1–O1	65.82(6)
O2–Mn1–O3	55.55(10)	N2–Mn1–N1	68.53(6)
O2–Mn1–O1	82.55(9)	O2–Mn1–N6	68.77(6)
N1–Mn1–O3	83.57(11)	O1–Mn1–N6	77.95(6)
O8–Mn1–N1	88.12(11)	O3–Mn1–O2	82.75(8)
O8–Mn1–N2	90.38(12)	O3–Mn1–N2	93.79(8)
O8–Mn1–O1	89.13(11)	O3–Mn1–N1	83.28(7)
O8–Mn1–O3	90.52(12)	O3–Mn1–O1	112.94(7)
O8–Mn1–O2	91.93(11)	O3–Mn1–N6	89.88(8)

3. 2. X-ray Crystallographic Analysis

Complex **1** crystallized in the triclinic space group $P\bar{1}$. L_1 serves as tridentate chelating ligand, the pyrimidine N-atom from nicotinoylhydrazine is not implicated in complexation. The coordination geometry around the

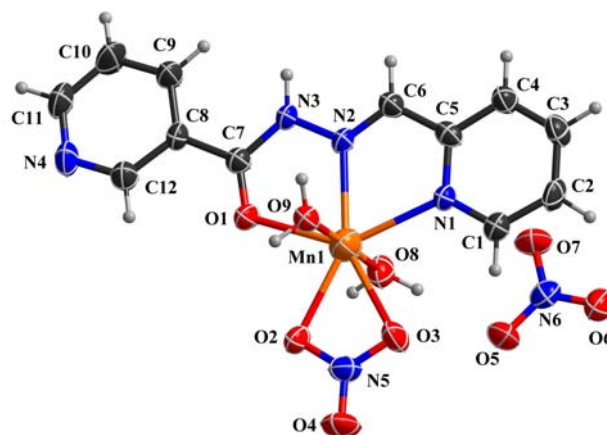


Figure 1. Molecular diagram for complex **1** showing the atom-labelling scheme (non-hydrogen) (50% thermal ellipsoids)

Mn(II) center is highly regular pentagonal bipyramid (Figure 1). The equatorial plane is surrounded by two O-atom donors (O2 and O3) from anion NO_3^- , one carbonyl O-atom (O1), one imine N-atom (N2) and one pyrimidine N-atom (N1) donors from L_1 , while the axial positions are occupied by O-atom donors (O8 and O9) from two coordinated water molecules. The bond angle of O9–Mn1–O8, $177.49(11)^\circ$, indicates that the three atoms are in good linear configuration. In addition, the sum of the equatorial angles O1–Mn1–N2, N2–Mn1–N1, N1–Mn1–O3, O3–Mn1–O2 and O2–Mn1–O1 for complex **1** ($\approx 360.09^\circ$) is very close to the ideal value (360.00°), which ensures the planarity of equatorial plane. The axial Mn–O average distance (2.188 \AA) is shorter than the equatorial Mn–O average distance (2.329 \AA) and Mn–N average distance (2.300 \AA), showing the squashed bipyramid surrounding the Mn(II) center. Compared with the salen-Mn complexes, the Mn–O_{carbonyl} bond length ($2.354(3) \text{ \AA}$) is obviously longer than the Mn–O_{phenolate} bond length ($1.850(2) \text{ \AA}$),²⁰ and Mn–N_{imine} bond length ($2.267(3) \text{ \AA}$) in complex **1** is also longer than that in salen-Mn complexes.^{20,21}

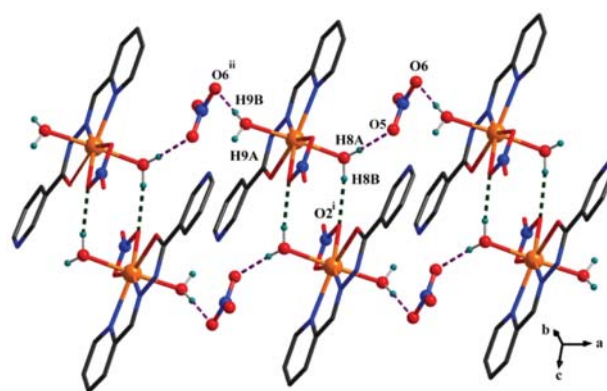


Figure 2. The hydrogen-bond-driven 1D chain extended in crystallographic a axis of **1**. [Symmetry codes: (i) $-x + 1, -y, -z + 1$; (ii) $x - 1, y, z$]

Since the anionic moieties NO_3^- possess the hydrogen bond acceptors²² and the water molecules possess the hydrogen bond donors,²³ complex **1** presents enhanced hydrogen-bonding framework in the solid state (Table 3). The adjacent mononuclear cations are seized together through the strong hydrogen bonding interactions ($\text{O8-H8B}\cdots\text{O2}^i$, symmetry code: (i) $-x + 1, -y, -z + 1$) between coordinated water molecules and NO_3^- into a 8-membered dimeric unit with the $\text{Mn}\cdots\text{Mn}$ separation of 5.407(1) Å. As shown in Figure 2, the free nitrate anions are located between these dimeric units, and serve as hydrogen bonding acceptor linking these dinuclear units into infinite double-chain structures along *a* axis via $\text{O8-H8A}\cdots\text{O5}$ and $\text{O9-H9B}\cdots\text{O6}^{ii}$ (symmetry code: (ii) $x - 1, y, z$) hydrogen bonds. These supramolecular chains stack in a face-to-face fashion in *ac* plane, the hydrogen

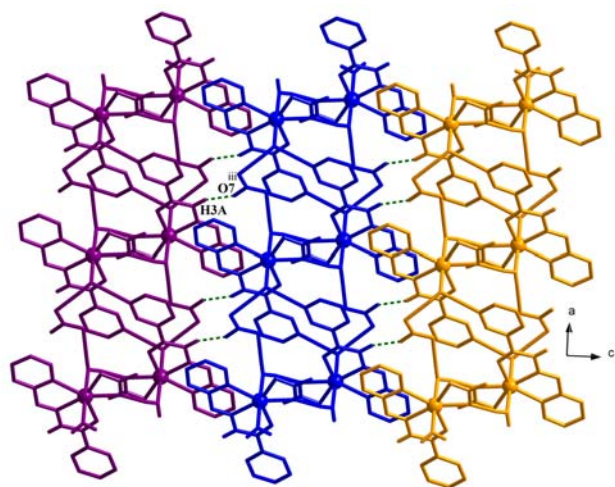


Figure 3. The hydrogen-bond-driven 2D sheet of **1** extended in crystallographic *ac* plane. [Symmetry codes: (iii) $-x + 1, -y, -z$]

bonds exist between the amido group of ligand L_1 and the oxygen atom of free nitrate to form an intermolecular $\text{N3-H3A}\cdots\text{O7}^{iii}$ (symmetry code: (iii) $-x + 1, -y, -z$) hydrogen bonding interaction, leading to the construction of 2D supramolecular sheet in the *ac* plane (Figure 3).

The idea behind the use of ligand L_2 is to control supramolecular motifs through a 4-pyridine-type ligand. It is known that the relative different orientation of the nitrogen donors on the pyridyl rings could result in unusual building blocks, which can lead to the construction of versatile supramolecular motifs. Crystallization of L_2 with $\text{Mn}(\text{NO}_3)_2$ for the self-assembly reaction in the $\text{CH}_2\text{Cl}_2/\text{EtOH}$ solvent system afforded $[\text{Mn}(L_2)_2(\text{NO}_3)(\text{H}_2\text{O})]\text{NO}_3$ (**2**). Complex **2** also crystallized in triclinic

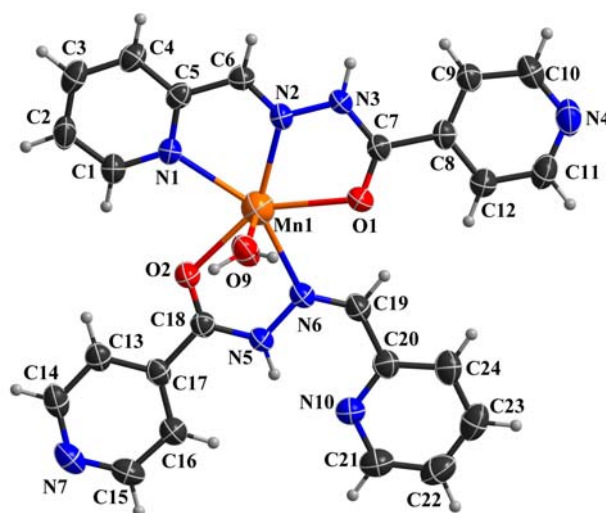


Figure 4. Molecular diagram for complex **2** showing the atom-labeling scheme (non-hydrogen, NO_3^- are omitted for clarity) (50% thermal ellipsoids).

Table 3. Geometrical parameters for hydrogen bonds

Hydrogen bonds	D–H (Å)	H \cdots A (Å)	D \cdots A (Å)	D–H \cdots A (°)
Complex 1				
$\text{O8-H8B}\cdots\text{O2}^i$	0.850(10)	1.918(11)	2.762(4)	172(4)
$\text{O9-H9B}\cdots\text{O6}^{ii}$	0.845(10)	2.008(14)	2.846(4)	171(5)
$\text{N3-H3A}\cdots\text{O7}^{iii}$	0.89	1.92	2.778(4)	160.3
$\text{O8-H8A}\cdots\text{O5}$	0.845(10)	2.065(12)	2.905(5)	173(4)
Complex 2				
$\text{O9-H9B}\cdots\text{N7}^{iv}$	0.84	1.96	2.801 (3)	171.7
$\text{O9-H9A}\cdots\text{O6}^v$	0.85	2.31	3.134 (4)	163.6
$\text{O9-H9A}\cdots\text{O8}^v$	0.85	2.33	2.929 (3)	127.7
$\text{N3-H3A}\cdots\text{O7}^{vi}$	0.888(10)	2.049(11)	2.930(3)	172(2)
$\text{N5-H5A}\cdots\text{N10}$	0.887(10)	1.908(19)	2.619(3)	136(2)

Symmetry transformations used to generate equivalent atoms: (i) $-x + 1, -y, -z + 1$; (ii) $x - 1, y, z$; (iii) $-x + 1, -y, -z$; (iv) $-x + 1, -y + 1, -z$; (v) $-x + 1, -y + 1, -z + 1$; (vi) $-x + 2, -y + 1, -z + 1$

space group $P\bar{1}$. An ORTEP view of **2** together with the atom numbering scheme is given in Figure 4. The complex **2** also showed pentagonal bipyramid geometry with a slight distortion as evidenced from the sum of five equatorial angles of 361.74° compared to the ideal value of 360° for planar geometry, and the axial O9–Mn1–O3 angle of $164.05(8)$ is also smaller than the ideal value of 180° . The Mn–O bond distance ($2.228(2)$ – $2.4148(16)$ Å) and Mn–N bond distance ($2.2894(18)$ – $2.3915(18)$ Å) are comparable to those found in complex **1**.

It is worthwhile to point out that the two L_2 ligands around the Mn center in complex **2** are crystallographic different. In one ligand, L_2 acts as tridentate NNO pincer type chelators, the C7=N3 bond defines the *E*-isomeric form where the two pyridine rings are *trans* to each other with the dihedral angle of $15.52(6)^\circ$. While in the second L_2 ligand, the two pyridine rings are *cis* to each other corresponding to C19=N6 bond, the dihedral angle between them is only $4.21(6)^\circ$. In this case, L_2 acts as bidentate NO chelating ligand.

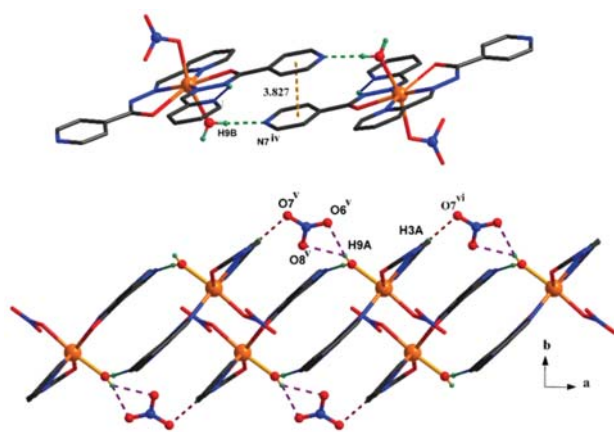


Figure 5. (a) The dimer structure of **2**. (b) The hydrogen-bond-driven 1D chain extended in crystallographic *a* axis of **2**. [Symmetry codes: (iv) $-x + 1, -y + 1, -z$; (v) $-x + 1, -y + 1, -z + 1$; (vi) $-x + 2, -y + 1, -z + 1$]

The crystal packing of complex **2** is stabilized by means of hydrogen bonding (Table 3) in combination with π – π stacking interactions. Similar to complex **1**, in complex **2**, as shown in Figure 5a, the adjacent molecules are linked through hydrogen bonding interactions to form dimers with Mn...Mn separation of $10.562(6)$ Å. The intermolecular hydrogen bond exists between the hydroxyl group of coordinated H_2O molecules and nitrogen atom of pyridine ring (O9–H9B...N7^{iv}, symmetry code: (iv) $-x + 1, -y + 1, -z$). Meanwhile, the centroid-to-centroid separation of two parallel pyridyl rings is found to be 3.827 Å, which indicates moderately strong π – π interactions. Strong intramolecular hydrogen bonding interactions N5–H5A...N10 are also observed in the dimer. The uncoordinated nitrate anions are located between these di-

meric units, and engaged in hydrogen bonding with coordinated H_2O molecules (O9–H9A...O6^v, O9–H9A...O8^v, symmetry code: (v) $-x + 1, -y + 1, -z + 1$) and amido groups (N3–H3A...O7^{vi}, symmetry code: (vi) $-x + 2, -y + 1, -z + 1$), giving rise to the double-chain supramolecular structure of complex **2** along *a* axis (Figure 5b).

3. 3. IR Spectroscopy

The spectra of complexes **1** and **2** exhibit broad bands at 3350 and 3383 cm^{-1} , respectively, which can be attributed to $\nu(OH)$ of the crystallized water molecules, and sharp peaks at 1556 and 1553 cm^{-1} , respectively, due to H–O–H bending vibrations.²⁴ The characteristic $\nu(NH)$ stretches are shown at 3220 cm^{-1} for **1** and 3178 cm^{-1} for **2**.²⁵ The sharp absorption bands of NO_3^- in **1** are clearly visible at 1381 and 823 cm^{-1} , while in **2** are at 1384 and 850 cm^{-1} .²⁶ In the complexes **1** and **2**, the involvement of the carbonyl O and azomethine N in coordination with Mn atom weakens the C=O band and C=N bond leads to the $\nu(C=O)$ and $\nu(C=N)$ towards lower frequencies in the region of ca. 1648 cm^{-1} and 1598 cm^{-1} , respectively.²⁴

3. 4. SOD Mimetic Property

Interest in Mn(II) complexes has been amplified due to their application in biology,^{15,27} e.g., Mn-MRI (magnetic resonance imaging) contrast, Mn-fluorescence agent, and Mn-SOD biomimetics. In previous reports, Mn(II) complexes of pentagonal bipyramidal geometry are functional mimics of SOD.^{14,15,28} In this paper, we studied the SOD mimetic activity of complexes **1** and **2**. The reported manganese complexes with various organic ligands (such as macrocyclic penta-amine, tripodal polyimidazole, di-Schiff base) showed IC_{50} values rank from 0.30 to 35 μM .^{14,29} In our study, **1** and **2** possess moderate activity of dismutation of superoxide with IC_{50} values of 32.5 and 21.0 μM , respectively. The IC_{50} values reported here are much larger than those of Mn(II) complex generated from di-Schiff base ligand (2.85 μM).¹⁴ This one order of magnitude difference may be ascribed to the rigid planar structure of **1** and **2**, which possess small tendency to fold.²⁸ Therefore the Mn(II) center is constrained in a geometry that limits fast electron-transfer, i.e., a pseudo octahedral geometry preferred by Mn(III).

4. Conclusion

In summary, nicotinoylhydrazine and isonicotinoylhydrazine were used to synthesize hydrazone Schiff base ligands L_1 and L_2 . Further coordination reactions of these ligands with $Mn(NO_3)_2$ afforded mononuclear complexes **1** and **2**, respectively. Although L_1 and L_2 are potential $NNNO$ tetradentate ligands, in complexes **1** and **2**,

they serve as *NNO* tridentate or *NO* bidentate chelating ligands. The N-donors free of coordination are engaged in constructing supramolecular architecture. This study demonstrates that the orientation of N_{pyridine} and hydrogen bonding patterns of nitrate anions play an important role in constructing unusual supramolecular compounds. Both of the two complexes exhibit moderate SOD mimetic activity.

5. Supplementary Information

CCDC files 1023096 (1) and 1023097 (2) contain the supplementary crystallographic data for this paper. These data can be obtained free of charge from The Cambridge Crystallographic Data Centre via www.ccdc.cam.ac.uk/data_request/cif.

6. Reference

1. A. Escuer, B. Cordero, M. Font-Bardia, T. Calvet, *Inorg. Chem.* **2010**, *49*, 9752–9754. <http://dx.doi.org/10.1021/ic101636r>
2. Y. B. Dong, X. Zhao, R. Q. Huang, *Inorg. Chem.* **2004**, *43*, 5603–5612. <http://dx.doi.org/10.1021/ic049787a>
3. R. Vafazadeh, M. Alinaghi, A. C. Willis, A. Benvidi, *Acta Chim. Slov.* **2014**, *61*, 121–125.
4. D. S. Kalinowsk, P. C. Sharpe, P. V. Bernhardt, D. R. Richardson, *J. Med. Chem.* **2008**, *51*, 331–344. <http://dx.doi.org/10.1021/jm7012562>
5. M. X. Li, L. Z. Zhang, D. Zhang, B. S. Ji, J. W. Zhao, *Eur. J. Med. Chem.* **2011**, *46*, 4383–4390. <http://dx.doi.org/10.1016/j.ejmech.2011.07.009>
6. P. G. Cozzi, *Chem. Soc. Rev.* **2004**, *33*, 410–421. <http://dx.doi.org/10.1039/b307853c>
7. T. Katsuki, *Chem. Soc. Rev.* **2004**, *33*, 437–444. <http://dx.doi.org/10.1039/b304133f>
8. H. Keypour, M. Shayesteh, M. Rezaeivala, F. Chalabian, Y. Elerman, O. Buyukgungor, *J. Mol. Struct.* **2013**, *1032*, 62–68. <http://dx.doi.org/10.1016/j.molstruc.2012.07.056>
9. D. Barut, N. Korkmaz, S. T. Astley, M. Aygün, *Acta Chim. Slov.* **2015**, *62*, 88–94.
10. S. Mondal, S. Naskar, A. K. Dey, E. Sinn, C. Eribal, S. R. Herron, S. K. Chattopadhyay, *Inorg. Chim. Acta* **2013**, *398*, 98–105. <http://dx.doi.org/10.1016/j.ica.2012.12.018>
11. P. S. Mukherjee, S. Dalai, E. Zangrando, F. Lloret, N. R. Chaudhuri, *Chem. Commun.* **2001**, 1444–1445. <http://dx.doi.org/10.1039/b104649g>
12. D. B. Dang, H. Gao, Y. Bai, X. J. Pan, W. L. Shang, *J. Mol. Struct.* **2010**, *969*, 120–125. <http://dx.doi.org/10.1016/j.molstruc.2010.01.051>
13. D. Salvemini, C. Muscoli, D. P. Riley, S. Cuzzocrea, *Pulm. Pharmacol. Ther.* **2002**, *15*, 439–447. <http://dx.doi.org/10.1006/pupt.2002.0374>
14. X. M. Ouyang, B. L. Fei, T. Okamura, W. Y. Sun, W. X. Tang, N. Ueyama, *Chem. Lett.* **2002**, 362–363. <http://dx.doi.org/10.1246/cl.2002.362>
15. D. P. Riley, *Chem. Rev.* **1999**, *99*, 2573–2587. <http://dx.doi.org/10.1021/cr980432g>
16. Y. F. Liu, Y. P. Liu, K. K. Zhang, Q. L. Ren, J. Qin, *Acta Cryst.* **2015**, *C71*, 116–121.
17. Bruker, *SMART and SAINT*, Bruker AXS Inc., Madison, Wisconsin, USA. **2002**.
18. G. M. Sheldrick, *SADABS, Program for Empirical Absorption Correction of Area Detector*, University of Göttingen, Germany **1996**.
19. G. M. Sheldrick, *Acta Crystallogr. A* **2008**, *64*, 112–122. <http://dx.doi.org/10.1107/S0108767307043930>
20. C. N. Chen, D. G. Huang, X. F. Zhang, F. Chen, H. P. Zhu, Q. T. Liu, C. X. Zhang, D. Z. Liao, L. C. Li, L. C. Sun, *Inorg. Chem.* **2003**, *42*, 3540–3548. <http://dx.doi.org/10.1021/ic025944z>
21. H. L. Shyu, H. H. Wei, Y. Wang, *Inorg. Chim. Acta* **1999**, *290*, 8–13. [http://dx.doi.org/10.1016/S0020-1693\(99\)00089-4](http://dx.doi.org/10.1016/S0020-1693(99)00089-4)
22. R. Custelcean, B. A. Moyer, V. S. Bryantsev, B. P. Hay, *Cryst. Growth Des.* **2006**, *6*, 555–563. <http://dx.doi.org/10.1021/cg0505057>
23. J. Qin, L. Cui, *Inorg. Chem. Commun.* **2013**, *36*, 170–173. <http://dx.doi.org/10.1016/j.inoche.2013.08.034>
24. A. A. El-Sherif, M. R. Shehata, M. M. Shoukry, M. H. Barakat, *Spectrochim. Acta A* **2012**, *96*, 889–897. <http://dx.doi.org/10.1016/j.saa.2012.07.047>
25. S. Mondal, S. Naskar, A. K. Dey, E. Sinn, C. Eribal, S. R. Herron, S. K. Chattopadhyay, *Inorg. Chim. Acta* **2013**, *398*, 98–105. <http://dx.doi.org/10.1016/j.ica.2012.12.018>
26. J. Qin, N. Lei, H. L. Zhu, *J. Coord. Chem.* **2014**, *67*, 1279–1289. <http://dx.doi.org/10.1080/00958972.2014.909591>
27. K. S. Dube, T. C. Harrop, *Dalton Trans.* **2011**, *40*, 7496–7497. <http://dx.doi.org/10.1039/c1dt10579e>
28. K. Aston, N. Rath, A. Naik, U. Slomeczynska, O. F. Schall, D. P. Riley, *Inorg. Chem.* **2001**, *40*, 1779–1789. <http://dx.doi.org/10.1021/ic000958v>
29. M. P. Clares, S. Blasco, M. Inclán, L. del C. Agudo, B. Verdejo, C. Soriano, A. Doménech, J. Latorre, E. García-España, *Chem. Commun.* **2011**, *47*, 5988–5990. <http://dx.doi.org/10.1039/c1cc10526d>

Povzetek

Dva nova liganda, potencialno štirivezni Schiffovi bazi, N' -(piridin-2-ilmetilen)nikotinohidrazide (L_1), in N' -(piridin-2-ilmetilen)izonikotinohidrazid (L_2) sta bila sintetizirana. Pri reakciji hidrazonskega liganda L_1 oziroma L_2 z $Mn(NO_3)_2$ nastaneta dva enojedrna Mn(II) kompleksa, $[Mn(L_1)(NO_3)(H_2O)_2]NO_3$ (**1**) in $[Mn(L_2)_2(NO_3)(H_2O)]NO_3$ (**2**). Pri spojinah **1** in **2** sta L_1 in L_2 tri- oziroma dvovezna liganda. Centralna Mn(II) iona sta v obeh spojinah heptakoordinirana, supramolekularna struktura v kristalu pa je pri spojinah zelo različna zaradi različne orientacije N_{piridin} in vodikovih vezi, v katerih sodeluje nitratni anion. Struktura **1** vsebuje 2D supramolekularne plasti, medtem ko ima struktura **2** motiv dvojne verige. Obe spojini izkazujeta zmerno superoksid dismutasno (SOD) mimetično aktivnost.

Electronic Supplementary Information

**Synthesis, Structural Diversity and Mimic Superoxide Dismutase of Mn(II)
Complexes Derived from N, O-donor Schiff-bases**

Jie Qin^{*}, Qiang Yin, Shan-Shan Zhao, Jun-Zheng Wang, Shao-Song Qian^{*}

School of Life Sciences, Shandong University of Technology, Zibo 255049, P. R. China

^{}Corresponding authors: Jie Qin, E-mail: qinjietutu@163.com*

Shao-Song Qian, E-mail: sdutqss@163.com

Tel.: 0086-533-2780271; Fax: 0086-533-2781329.

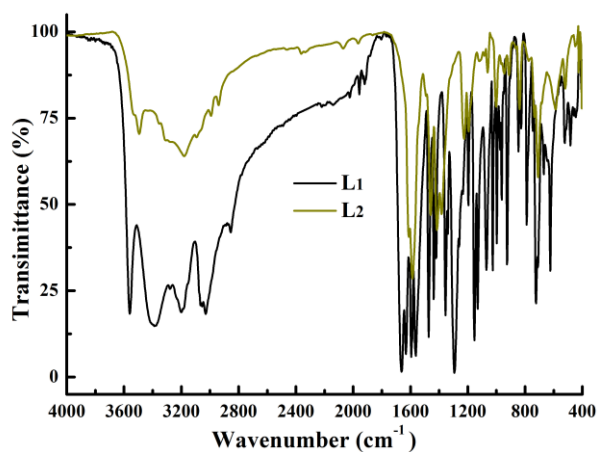


Figure S1 IR spectra of ligands L₁ and L₂.

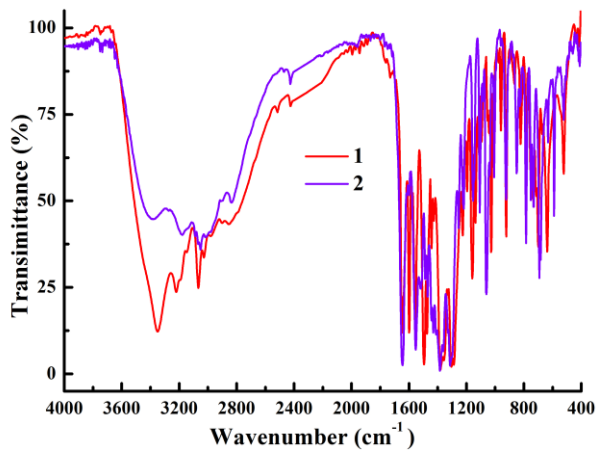


Figure S2 IR spectra of complexes 1 and 2.

